

Temperature Dependence of the EPR Spectra of Niobium-Doped TiO_2 [†]

Peter H. Zimmermann*

Department of Physics, University of California, Los Angeles, California 90024

(Received 14 May 1973)

Detailed measurements of the temperature dependence of the EPR spectrum and Hall coefficient of niobium-doped rutile have been made. At 4.2 °K and 34 GHz, the EPR spectrum consists of a set of well-resolved hyperfine lines which coalesce and then shift with increasing temperature. Computer calculations of explicit line shapes have been performed based on a model of random hopping between donor sites. Direct impurity-impurity and impurity-conduction-band-impurity hopping are discussed. The hopping frequency is found to vary exponentially with temperature. The temperature dependence is proportional to that of the conduction-electron concentration and is attributed to exchange scattering of the donor electrons with the conduction electrons. The exchange-scattering cross section is found to equal $\sigma_{ex} = 3 \times 10^{-15} \text{ cm}^2$.

I. INTRODUCTION

The electron-paramagnetic-resonance spectrum of Nb-doped TiO_2 (rutile) at 9 GHz has been reported by Chester.¹ His experimental results indicate that the niobium occupies substitutional Ti^{4+} sites in the form of $\text{Nb}^{4+}(4d^1)$. At 4.2 °K, a ten-line hyperfine spectrum is observed for each of the two inequivalent substitutional sites. These are appropriate to the $I = \frac{5}{2}$ nuclear moment of Nb^{93} (100% natural abundance) and can be fitted to a simple spin Hamiltonian.

Chester provided additional qualitative information on the temperature dependence of the hyperfine spectrum. He found the features essentially unchanged up to about 25 °K, above which temperature the lines gradually coalesced into a single narrowed line.

This work presents a more complete investigation and interpretation of the temperature dependence of the spectrum in the coalescing regime. Together with detailed EPR measurements at 34 GHz, the Hall coefficient has also been measured. This allows for a direct measure of the conduction-electron concentration, assisting in the interpretation of the EPR spectrum.

II. EXPERIMENTAL

All rutile samples were cut from a single boule grown by the National Lead Co. with a nominal niobium concentration of 0.04 at.%. The color of the boule appeared dark blue; thin (1-mm) slabs were a medium blue.

The boule was oriented by Laue x-ray scattering. After orientation, samples were cut from the boule with a diamond saw and when necessary ground to the final shape with a lapping machine. The EPR samples were of cubical shape with sides approximately 1 mm in length. The faces were the [001] and $[1\bar{1}0]$ crystalline planes. One sample was cleaved in the $[110]$ plane and was used for all

final measurements.

Hall samples were cut to the shape of a rectangular prism about $17 \times 1.2 \times 0.8$ mm in dimension. The current was in the direction of the [001] prism axis, while the magnetic field was in the $[110]$ direction. Electrical contacts were made with indium using an ultrasonic soldering iron.

The EPR measurements were made with a conventional reflection type spectrometer in conjunction with a Varian 12-in. electromagnet. Calibration of the Nb^{4+} concentration was done at 9.5 GHz and 4.2 °K. The rutile sample was mounted inside of a cylindrical cavity next to the Varian standard, 0.01% pitch in KCl. By observing and comparing the power absorption (not the derivative) of the two samples, the Nb^{4+} concentration was obtained as $c = 3.6 \times 10^{18} \text{ cm}^{-3}$.

All other EPR measurements were made with a cylindrical microwave cavity operating at 34 GHz. Since the Nb^{4+} hyperfine spectra arising from the two types of inequivalent sites in rutile have different g factors for arbitrary directions of the magnetic field, operating at 34 GHz had the advantage of giving a large separation between these spectra, as compared to 9 GHz. The sample temperature was varied by mounting it on a substrate, whose temperature was maintained by a heater in conjunction with an electronic feedback system. The microwave cavity was surrounded by an evacuated can, which in turn was immersed in a liquid-helium bath. Temperature measurements were made with a Cryocal, Inc. germanium resistor. Shifts of the cavity resonant frequency with temperature were less than $0.1 \text{ MHz}/^\circ\text{K}$, which corresponds to a maximum error of 1.7 G in the determination of the resonance line positions.

Measurements of the Hall effect were made by gluing the rutile samples to a copper block inside an evacuated can which could be immersed in a liquid-helium or liquid-nitrogen bath. The temperature of the copper block was again regulated by

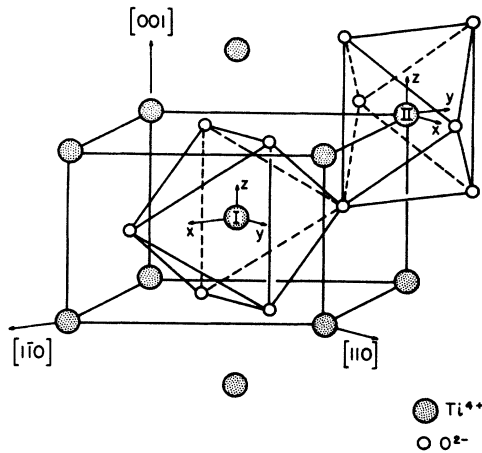


FIG. 1. Crystal structure of rutile (TiO_2). The two inequivalent sites are labeled I and II, and their magnetic axes are labeled x , y , and z .

a heater and measured with a germanium resistor. Hall voltages were measured with a Fluke 895A dc differential voltmeter. In this manner measurements were undertaken between 7 and 100 °K. Below 7 °K the sample resistivity became too high for accurate measurement. At 200 °K measurements were taken by immersing the sample in a mixture of powdered dry ice and transformer oil, room temperature was stabilized by immersion in transformer oil alone.

III. EXPERIMENTAL RESULTS

The crystal structure of rutile is tetragonal (D_{4h}^{14}) with two titanium atoms per unit cell. These two sites have orthorhombic point symmetry (D_{2h}) and are equivalent except for a 90° rotation about the c axis, as shown in Fig. 1. The EPR spectra corresponding to the two inequivalent sites merge into a single spectrum for $\vec{H} \parallel \hat{c}$ and $\vec{H} \parallel \hat{a}$.

Following Chester,¹ we write the spin Hamiltonian for a particular substitutional site as

$$\begin{aligned} \mathcal{H} = & \mu_B (g_x H_x S_x + g_y H_y S_y) + A_x S_x I_x \\ & + A_y S_y I_y + \frac{3}{2} P_x [I_x^2 - \frac{1}{3} I(I+1)] \\ & + \frac{1}{2} (P_x - P_y) (I_x^2 - I_y^2) - g_n \mu_N \vec{H} \cdot \vec{I}, \quad (1) \end{aligned}$$

where we have labeled the magnetic axes $[1\bar{1}0]$, $[110]$, and $[001]$ of a Ti^{4+} substitutional sites as x , y , and z , respectively. For a magnetic field parallel to any of these three directions, the hyperfine spacing was regular to within experimental error. Therefore, the terms containing P in Eq. (1) can be neglected. With $\vec{H} \parallel [001]$, both sites gave rise to a single ten-line hyperfine spectrum, clearly resolved at 4.2 °K. The features of the spectrum remained essentially unchanged up to ~17 °K. As the temperature was increased fur-

ther, the hyperfine lines gradually coalesced until only a single line was observed at ~25 °K [Fig. 2(a)]. Above this temperature, the signal became increasingly dispersive, which is characteristic of conducting materials.^{2,3} Analysis of the line shape by the method of Peter *et al.*⁴ showed that the line shifted towards higher magnetic field with increasing temperature. The maximum shift was 11 G at 48 °K, which is the largest temperature for

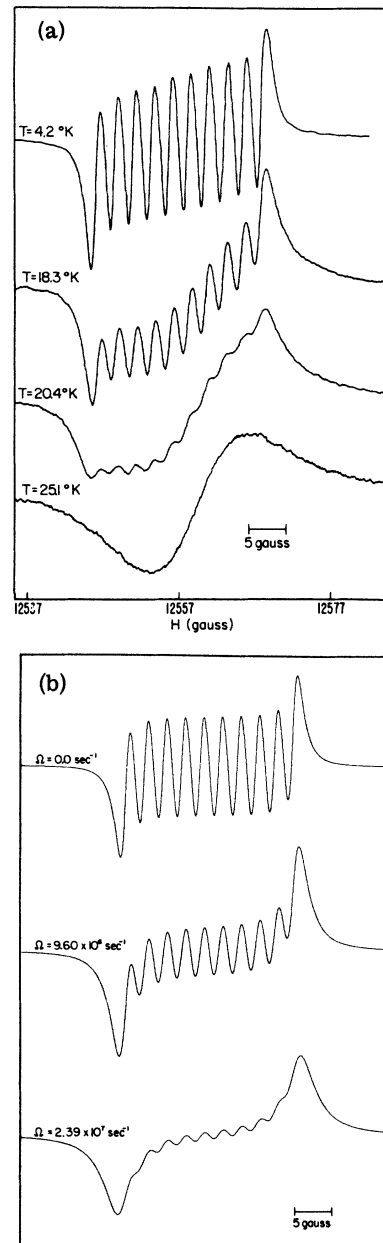


FIG. 2. (a) Experimental EPR spectra of Nb-doped rutile with $\vec{H} \parallel [001]$ at various temperatures is shown. The corresponding computer calculated curves that best fit the three low-temperature spectra are shown in (b).

which the signal could be clearly resolved. The width of this single line decreased with increasing temperature to a minimum of 10 G at 34 °K, then broadened to about 22 G at 48 °K.

For $\vec{H} \parallel [110]$, the hyperfine spectra corresponding to $\vec{H} \parallel \hat{x}$ and $\vec{H} \parallel \hat{y}$ of the two inequivalent sites were observed [Figs. 3(a) and 3(c)]. Although these spectra completely overlap each other at 9 GHz, they are almost separated at 34 GHz and 4.2 °K. The $\vec{H} \parallel \hat{x}$ spectrum behaved similar to

the $\vec{H} \parallel \hat{z}$ spectrum described above; the coalescing of the hyperfine lines occurred at a slightly lower temperature with merging into a single line already complete at ~ 21 °K. As the temperature was increased further, this line was observed to shift towards *lower* magnetic field. Simultaneously, the line broadened to a value of 20 G at 51 °K. (See Figs. 6 and 7.) Decreasing of the signal-to-noise ratio prevented observation of this signal at higher temperatures.

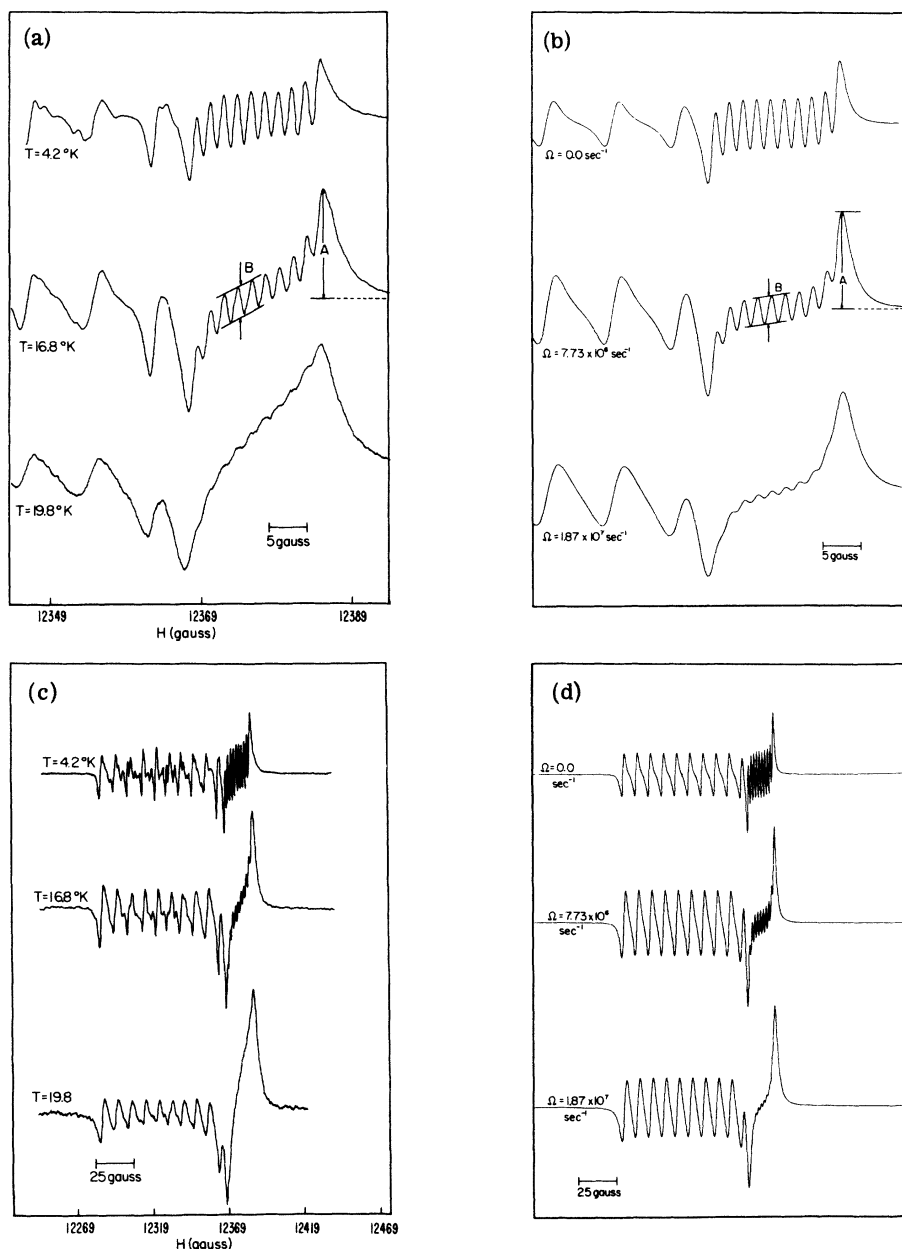


FIG. 3. Experimental EPR spectra for Nb-doped rutile [(a) and (c)] with $\vec{H} \parallel [110]$ at various temperatures, along with the best-fitting computer calculated curves [(b) and (d)]. The $\vec{H} \parallel \hat{y}$ and $\vec{H} \parallel \hat{x}$ spectra are at lower and higher values of magnetic field, respectively.

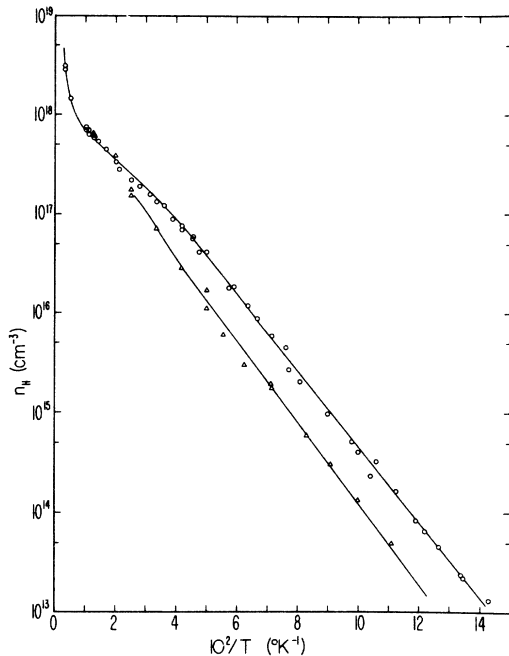


FIG. 4. Number of Hall carriers n_H in Nb-doped rutile as a function of inverse temperature. The two curves are the results for different regions of the boule.

The hyperfine spacing of the $\vec{H} \parallel \hat{y}$ spectrum was much larger with some partially resolved structure at 4.2 °K [Fig. 3(c)]. This structure can be attributed to $\Delta m_I = \pm 1$ transitions which are allowed through the electric quadrupole interaction if the magnetic field is not oriented along one of the principal axes of the crystal. Only slight misalignment can give rise to "forbidden" transitions of considerable intensity; in fact, their appearance has been used as a very sensitive method of orientation for $\text{TiO}_2:\text{Cu}$.⁵ Unfortunately, the small size of our samples, which were fixed inside of the cavity, made precise orientations difficult to achieve.

A very gradual broadening of the individual lines of this spectrum was observed in the 18–25 °K temperature region. Most of the hyperfine lines could still be resolved at 25 °K, but there was appreciable overlap with the tail of the much larger $\vec{H} \parallel \hat{x}$ absorption derivative signal near this temperature. Decreasing signal-to-noise ratio and further broadening prevented observation of the $\vec{H} \parallel \hat{y}$ spectrum at higher temperatures.

Hall measurements were made on several different regions of the boule between 7 and 300 °K. The results obtained are typical of data on doped and reduced rutile taken by previous authors^{6–8} in that two regions with different activation energies can be distinguished. The temperature dependence of the number of Hall carriers at low temperatures

is given by $n_H \propto T^{3/2} e^{-E_a/kT}$,⁹ where E_a is the depth of the donor level below the conduction band. From the slope of a plot of $\ln(T^{-3/2}n_H)$ vs $1/T$ the activation energy below 40 °K was found to be $E_a/k = 72$ °K, while above 200 °K a much higher activation energy is appropriate.

Results for two different regions of the boule are shown in Fig. 4. It can be seen that different values of the Hall coefficient were obtained in the low-temperature region, with activation energies identical to within experimental error. Such a variation of the Hall coefficient is an indication of macroscopic impurity inhomogeneity in the boule. This inhomogeneity cannot be traced to a spacial variation of the Nb^{4+} concentration, since no such variation was found in the Nb^{4+} absorption intensity of samples cut from the Hall bars at 4.2 °K.

IV. INTERPRETATION

A. Hopping Model

Because a narrowed line is observed ($\vec{H} \parallel \hat{z}$) in the high-temperature region, the coalescing of the hyperfine lines can certainly not be attributed solely to a temperature dependent increase in the line-width (e.g., spin-lattice relaxation). Instead, we attribute the changes of line shape and the shifts to a line-hopping mechanism and interpret them in terms of Anderson's model of "random frequency modulation."¹⁰ Two processes may contribute¹¹: (i) thermal excitation of the $4d^1$ donor electrons to the conduction band and (ii) exchange scattering of the donor electrons with the conduction electrons. Either process results in the hopping of electrons from one donor site to another via the conduction band. Thus, electrons successively "feel" the hyperfine field of the first Nb-donor nucleus, the conduction electrons, and then the hyperfine field of the second donor. Since the nuclear orientation of each donor is random, the net effect is that of hopping from one hyperfine line to the conduction electron resonance line, and then back to any of the hyperfine lines of the spectrum. If the hopping is faster than the hyperfine frequency separation of the resonance lines, the spectrum will first coalesce and then narrow. Depending on the relaxation time and resonance position of the conduction electrons, the spectrum may also shift or broaden.

To calculate the exact line shapes, we turn to the results of Anderson,^{10,12} who finds that the absorption spectrum is given by

$$I(\omega) = -\text{Re}(\underline{W} \cdot \underline{A}^{-1} \cdot \underline{1}),$$

where $\underline{1}$ is a vector with components of unity, \underline{W} a vector whose components are the absorption intensity of the individual resonance lines. The matrix \underline{A} is given by

$$\underline{A} = i(\underline{\omega} - \omega \underline{E}) - \underline{\delta} + \underline{\Pi},$$

where $\underline{\omega}$ is a diagonal matrix whose eigenvalues are the resonance frequencies ω_i , \underline{E} is the unit matrix, and $\underline{\delta}$ is a diagonal matrix with eigenvalues δ_i , the intrinsic linewidth of the i th resonance line without hopping. The only off-diagonal terms in \underline{A} are the hopping terms $\Pi_{ij} = \Pi(\omega_i, \omega_j)$, which give rise to the coupling of the resonance lines.

Applying the theory to $\text{TiO}_2:\text{Nb}^{4+}$, we have N hyperfine lines ($i=1, 2, \dots, N$); $N=10$, $\vec{H} \parallel [001]$; $N=20$, $\vec{H} \parallel [110]$ and the conduction-electron resonance line ($i=N+1$). Assuming hopping only between the donor Nb nuclei with particular but random values of m_I and the conduction band gives nonzero diagonal and furthest off-diagonal elements only for \underline{A} . Further assuming the hopping rate from the donors to the conduction band to be inde-

pendent of the nuclear orientation and denoting it by Ω gives

$$\Pi_{i,i} = -\Omega, \quad \Pi_{i,N+1} = \Omega, \quad i=1, 2, \dots, N.$$

Calling the inverse rate Ω' , we find that the only other nonvanishing matrix elements of $\underline{\Pi}$ are

$$\Pi_{N+1,N+1} = -\Omega', \quad \Pi_{N+1,i} = \Omega'/N, \quad i=1, 2, \dots, N.$$

Detailed balance is satisfied by requiring

$$\Delta \Omega' = (1 - \Delta)\Omega,$$

where Δ is the fraction of the electrons in the conduction band. We further set the absorption intensity of the i th line equal to the occupation, i. e.,

$$W_{N+1} = \Delta, \quad W_i = (1 - \Delta)/N; \quad i=1, 2, \dots, N.$$

With these assumptions we show in the Appendix that the absorption spectrum is calculated as

$$I(\omega) = -\text{Re} \left\{ \left(\frac{1-\Delta}{N} (A_{N+1,N+1} - \Omega) + \Delta \left[\left(\sum_{i=1}^N (A_{i,i})^{-1} \right)^{-1} - \frac{\Omega'}{N} \right] \left[A_{N+1,N+1} \left(\sum_{i=1}^N (A_{i,i})^{-1} \right)^{-1} - \frac{\Omega \Omega'}{N} \right]^{-1} \right) \right\}. \quad (2)$$

We explicitly exhibit the denominator of this expression, by rewriting it as

$$I(\omega) = -\text{Re} \left\{ \left(\frac{1-\Delta}{N} (A_{N+1,N+1} - \Omega) - \frac{\Delta \Omega'}{N} \left(\sum_{p=1}^N \prod_{i \neq p} A_{i,i} \right) + \Delta \prod_{i=1}^N A_{i,i} \right) \left(A_{N+1,N+1} \prod_{i=1}^N A_{i,i} - \frac{\Omega \Omega'}{N} \sum_{p=1}^N \prod_{i \neq p} A_{i,i} \right)^{-1} \right\}. \quad (3)$$

To gain insight into the properties of the spectrum, we proceed to consider several limits. In these considerations we closely adhere to the work of Barnes *et al.* who have investigated the poles of Eq. (3) in a discussion of the hyperfine splitting of localized magnetic moments in metals.¹³ Since for our experimental conditions $\Delta \ll 1$ (see Fig. 5), thus $\Omega' \gg \Omega$, our system is quite similar to the situation commonly found in metals.

It becomes useful to distinguish between two regimes: (i) the unbottlenecked regime and (ii) the bottlenecked regime. The unbottlenecked regime is obtained when $\delta_{\text{CE}} + \delta_i \gg \Omega + \Omega'$ or when $\omega_i - \omega_{\text{CE}} \gg \Omega + \Omega'$, where CE and i refer to the conduction electron and the hyperfine resonance lines, respectively. Calculations of Barnes *et al.* show that in this regime the hopping results in a simple broadening of the hyperfine spectrum, the width of the i th line becomes $\Omega + \delta_i$. This can be understood if we consider that, after hopping to the conduction band, an electron will relax to the lattice before hopping back to an impurity site or it will precess long enough in the conduction band so that it will hop back to an impurity site with arbitrary phase. Either case can be considered as a type of relaxation process of the impurities, leading to line broadening only. This point of view was also previously adopted in interpreting the line broadening of EPR spectra in transition-metal com-

pounds.^{14,15}

In the bottlenecked regime (reversal of both of the inequalities above) an electron will not relax to the lattice or dephase before hopping back to an impurity site. If, in addition, we impose the limit of vanishing conduction electron population, Ω' will be extremely rapid and the hopping process becomes identical to direct impurity-impurity hopping (see Appendix B), the conduction band acting as a sort of virtual state. Considering that $1/N$ on the electrons hopping to the conduction band will return to the same hyperfine line from which they originated, we obtain for slow hopping ($\Omega \ll |\omega_i - \omega_j|$) again a simple broadening of the hyperfine lines, the width of the i th line becoming $[(N-1)/N]\Omega + \delta_i$. If on the other hand the hopping is very fast such that $\Omega \gg \omega_i - \omega_j$, a single narrowed line with width $\bar{\delta}_i$ at $\bar{\omega}_i$ is obtained. Barnes *et al.* have shown that the effect of finite Δ (but still $\Delta \ll 1$) leads to a single line of width $(1-\Delta)\bar{\delta}_i + \Delta\delta_{\text{CE}}$ at $(1-\Delta)\bar{\omega}_i + \Delta\omega_{\text{CE}}$ for fast hopping, while for slow hopping the result is identical to direct impurity-impurity hopping.

B. Application of the Hopping Model

Because of the complexity of Eq. (2), numerical methods are the only feasible way of evaluating the spectra in the general case. We have performed numerical computations of the absorption derivative

TABLE I. Parameters for $\text{TiO}_2:\text{Nb}^{4+}$.

Direction of H	g^a	$A(10^{-4} \text{ cm}^{-1})^a$	$A(10^{-4} \text{ cm}^{-1})^b$	$\delta(\text{G})^c$
[001] (\hat{z})	1.948	2.1	2.32 ± 0.10	1.3
[1 $\bar{1}$ 0] (\hat{x})	1.973	≤ 1.8	1.66 ± 0.10	1.1
[110] (\hat{y})	1.981	8.0	7.93 ± 0.20	1.6

^aChester's values.

^bThis experiment.

^c δ are the Lorentzian linewidths of the hyperfine lines that best fit the 4.2°K spectra.

with aid of an IBM 360/91 computer, with results both in numerical and graphical form. Assuming Ω to increase with temperature, we can interpret all of the experimental results in terms of our hopping model.

As for numerical computations, all of the parameters in Eq. (2) must be known. The relative number of conduction electrons, Δ , was calculated by taking the conduction electron concentration from the Hall measurements and dividing it by the concentration of Nb^{4+} sites from the EPR calibration at 4.2°K. To determine the hyperfine parameters, we note that for zero hopping, Eq. (2) reduces to a superposition of Lorentzian lines

$$I(\omega) = -\text{Re} \left(\frac{1-\Delta}{N} \sum_{i=1}^N [-i(\omega - \omega_i) - \delta_i]^{-1} + \Delta [-i(\omega - \omega_{\text{CE}}) - \delta_{\text{CE}}]^{-1} \right). \quad (4)$$

Since the experimental spectra retain about the same shape up to 15°K, there is presumably no hopping at 4.2°K.

We match (4) to the experimental 4.2°K spectra and obtain the hyperfine line positions ω_i and their "intrinsic" width δ_i (see Table I). The equivalent parameters for the conduction electrons ω_{CE} and δ_{CE} are unknown, since their resonance could not be observed. Due to small carrier concentration and possible broad linewidth, observation of this resonance may be extremely difficult and to our knowledge no such observation has ever been reported.

Fortunately, lack of this information does not hamper interpretation in the lower temperature range, where the hyperfine lines are still partially resolved. Indeed, from the discussion in the last section we expect that the onset of hopping will result in line broadening only, both in the bottlenecked and unbottlenecked regimes, independent of the quantities ω_{CE} and δ_{CE} . Numerical calculations show that a simple line broadening is a good approximation to Eq. (2) for values of Ω small enough so that the individual hyperfine lines are resolved and for a wide variety of values of ω_{CE} and δ_{CE} . Very good agreement with the experimental spectra

is obtained (see Figs. 2 and 3). Since direct impurity-impurity hopping will also lead to line broadening for small hopping rates, we conclude that either it or impurity-conduction-band-impurity hopping adequately describe the experimental spectra in the lower temperature range.

Next we turn to a discussion of the spectra at higher temperatures at which the individual hyperfine lines are no longer resolved. For $\vec{H} \parallel \hat{z}$ the coalescing of the ten hyperfine lines into a single narrowed line was complete at 25°K [Fig. 2(a)]. With further increase in temperature this line was observed to narrow slightly more, and then to broaden, while the center of the line simultaneously shifted towards higher magnetic field. The narrowing can be explained in terms of increased coupling (hopping) between the individual hyperfine lines in the spirit of direct impurity-impurity hopping. However such coupling alone does not result in any shift or broadening. Thus a simple impurity-impurity hopping model fails at these temperatures and we turn to impurity-conduction-band-impurity hopping for interpretation.

With increasing temperature the coupling of the hyperfine lines with the conduction electrons is expected to become considerable, because of an increase in the relative number of conduction electrons Δ and in the hopping rate Ω . Such a coupling will shift and can broaden the line if the system is (at least partially) bottlenecked. The shift will be in a direction towards the conduction electron resonance, with a maximum value of $\Delta(\omega_{\text{CE}} - \bar{\omega}_i)$ in the extreme bottlenecked limit. Since the observed shift was towards higher field, we conclude that the conduction-electron g factor g_{CE} is less than g_{e} , i. e., $g_{\text{CE}} < 1.948$. A lower bound of the difference in the g factors can be estimated. Using the experimental values of the observed shift and of Δ at 50°K, we find $g_{\text{CE}} \lesssim 1.8$.

Lack of information of the band structure of rutile precludes a theoretical estimate of this quantity. However, such a value is reasonable in light of the wide variety of conduction electron g factors commonly found in semiconducting materials. For instance, values close to 1.8 have been reported for ZnS and CdS.¹⁶

Quantitative predictions of the broadening are difficult to make. We note that the smallest width that can be obtained from the hopping model is $\bar{\delta}_i$, corresponding to complete narrowing of the hyperfine lines. In the limit of large hopping the width becomes the weighted average $(1-\Delta)\bar{\delta}_i + \Delta\delta_{\text{CE}}$ in the bottlenecked regime, while the intermediate hopping regime can only be solved numerically. Considering that the system may not be completely bottlenecked and that part of the observed broadening may be due to an increase in the spin lattice relaxation rate, it is not possible to draw any

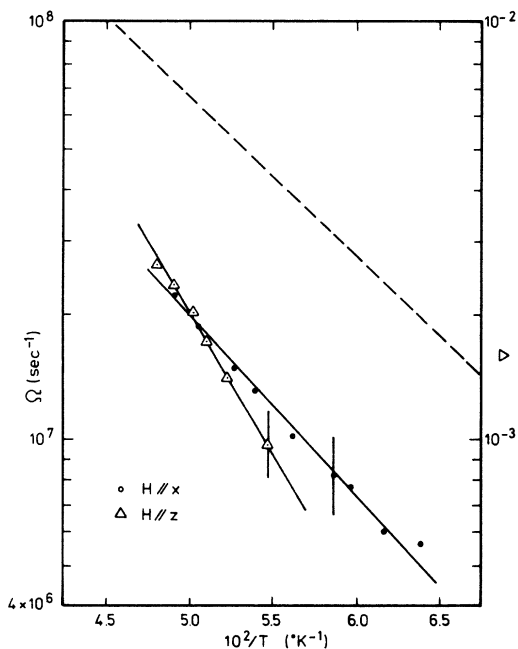


FIG. 5. Hopping frequency (solid lines) and the relative number of electrons in the conduction band (dashed line) in Nb-doped rutile as a function of inverse temperature.

quantitative conclusions from the broadening.

Turning to the $\vec{H} \parallel [110]$ spectrum, we note again that in the coalesced regime only the $\vec{H} \parallel \hat{x}$ spectrum could be well resolved, since the $\vec{H} \parallel \hat{y}$ spectrum was very broad and partially obscured by the tail of the $\vec{H} \parallel \hat{x}$ line. With increasing temperature this line was observed to shift towards lower field and to broaden. We attribute the shift to increasing coupling with the $\vec{H} \parallel \hat{y}$ spectrum competing with coupling to the conduction electrons, which tends to shift the line towards higher field. Assuming the latter effect the same as the observed shift for $\vec{H} \parallel \hat{z}$, we can separate the shift due to coupling with the $\vec{H} \parallel \hat{y}$ spectrum only, and find it to be ~ 30 G at 47°K . The maximum shift predicted by the hopping model is just one-half of the separation between the centers of the two low-temperature hyperfine spectra, i. e., 26 G. These values are in agreement to within experimental error and suggest that the line observed in the high-temperature limit for $\vec{H} \parallel [110]$ arises from the complete coupling of the $\vec{H} \parallel \hat{x}$ and $\vec{H} \parallel \hat{y}$ spectra. The broadening of this line is attributed to a combination of increase in coupling with the conduction electrons and to a possible increase in the spin-lattice relaxation rate, just as in the $\vec{H} \parallel \hat{z}$ case.

To gain quantitative information about the hopping rates, we turn back to the regime of resolved hyperfine structure. We obtain an estimate of the

temperature dependence of Ω by matching the computer calculated curves to the experimental spectra. As a sensitive criterion for matching, the ratio of the shoulders of the absorption derivative A to the amplitude of the central hyperfine lines B was chosen to characterize the spectra (see Fig. 3). Thus by comparing the A/B ratio of the computer calculated curves to those of the experimental spectra at many temperatures, we have obtained Ω as a function of temperature.

An Arrhenius plot of the results is shown in Fig. 5. The best fitting straight line¹⁷ to the points in the plot can be expressed in functional form as

$$\Omega = 4.9 \times 10^{10} e^{-156/T} \text{ sec}^{-1}, \quad \vec{H} \parallel \hat{z}$$

$$\Omega = 2.7 \times 10^9 e^{-98/T} \text{ sec}^{-1}, \quad \vec{H} \parallel \hat{x}.$$

We note that the temperature dependence of the hopping rate for $\vec{H} \parallel \hat{x}$ corresponds closely to that of the conduction electron population, but not for $\vec{H} \parallel \hat{z}$. However, we find that the expression

$$\Omega = (2.7 \pm 1.3) \times 10^9 e^{-(98 \pm 10)/T} \text{ sec}^{-1} \quad (5)$$

can be used to describe both the $\vec{H} \parallel \hat{x}$ and $\vec{H} \parallel \hat{z}$ results to within the error bars.

In principle, a determination of the temperature dependence of Ω could be made also for the $\vec{H} \parallel \hat{y}$ spectrum. At lower temperatures values of Ω could be obtained from measurements of the width of the individual hyperfine lines. At higher temperatures where the individual lines overlap, an analysis of the line shape just as for the other two spectra would be appropriate. Such an analysis, however, is not feasible for this experiment, since at lower temperatures the widths were obscured by appearance of the $\Delta m_I = \pm 1$ transitions, while at higher temperatures the signal was too noisy. To within experimental error, interpretation of the $\vec{H} \parallel \hat{y}$ spectrum is consistent with the assignment of Ω made for the other spectra.

C. Hopping Mechanism

Next we turn to a discussion of the physical origins of the hopping in the regime of resolved hyperfine structure where the hopping rate has been calculated from the EPR spectra (Fig. 5). Analysis of the hopping predicted by different processes will show that the dominant contribution to the hopping is exchange scattering with the conduction electrons. First, however, we investigate the other possible processes.

1. Direct Impurity-Impurity Hopping

Even though direct impurity-impurity hopping fails to explain the experimental results at high temperatures, previous considerations have shown that in the regime of resolved hyperfine structure, this process, under certain circumstances, affects

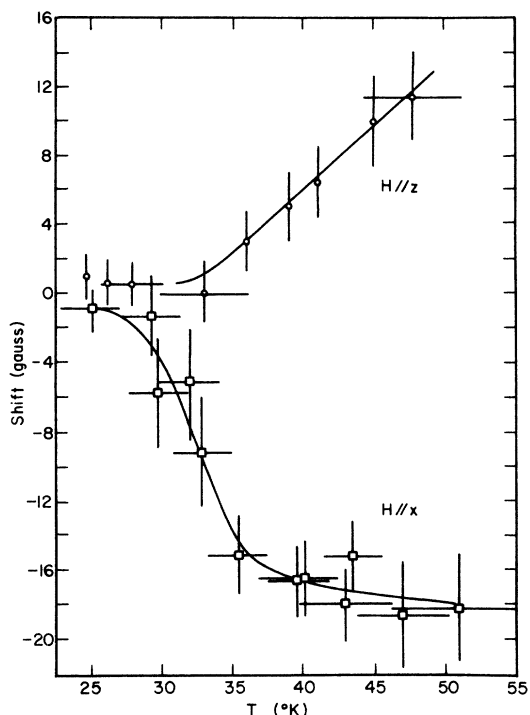


FIG. 6. Shift of the center of the hyperfine spectra of Nb-doped rutile as a function of temperature.

the spectra in a manner identical to hopping via the conduction band. Direct impurity-impurity hopping has been treated by Miller and Abrahams¹⁸ in connection with impurity conduction in elemental semiconductors at low concentrations. These authors consider phonon activated hopping, where electrons move between un-ionized and ionized donor sites by absorption or emission of a phonon. From their work we calculate that the temperature dependence of the direct hopping rate would be

$$\Omega_p \propto E_b [\coth(E_b/2kT) + 1], \quad (6)$$

where E_b is the energy barrier against the hopping process, arising from fluctuations of the local fields at different donor sites.

No values of E_b are available for rutile. In the elemental semiconductors values of E/k have been determined by EPR and range from 3 to 10°K.¹⁹⁻²¹ By using a nonlinear least-squares-fit computer program,¹⁷ we have found that it is impossible to match Eq. (6) to our data with values of $E_b/k \leq 80$ °K. The use of larger values of E_b seems unreasonable in light of the data for the other semiconductors. Since direct hopping also does not predict the observed spectra at higher temperatures, we conclude that this process is not an important effect.

2. Thermal Activation to Conduction Band

Two processes may induce hopping via the con-

duction band. The first is thermal activation of donor electrons to the conduction band by phonons. Kubo and Toyozawa²² have considered this problem and show that the temperature dependence is given by

$$\Omega_i \propto (kT/E_0)^2 e^{-E^*/kT},$$

where $E^* = E_0[(1 + \frac{1}{2}\alpha)^2/2\alpha]$, E_0 is the depth of the donors below the conduction band, and α is a constant associated with the electron-phonon interaction. We note that $E^* \geq E_0$ for any value of α . Since the temperature region of interest is rather small a plot of $\ln\Omega_i$ vs $1/T$ is nearly linear, with the magnitude of the slope being greater than E_0 .

Below 40°K the Hall measurements are characteristic of an activation energy of 72°K. Previous measurements²³ on niobium-doped rutile have shown an activation energy of 290°K in the low-temperature range. This leads us to believe that the depth E_0 of the Nb donors in rutile is at least 290°K and that the source of conduction electrons in our samples is due to some other (unknown) type of impurity. However, the measured temperature dependence of the hopping has an activation energy of (99 ± 10) °K, which is smaller than E_0 . Thus, we conclude that thermal activation to the conduction band cannot explain the observed effects.

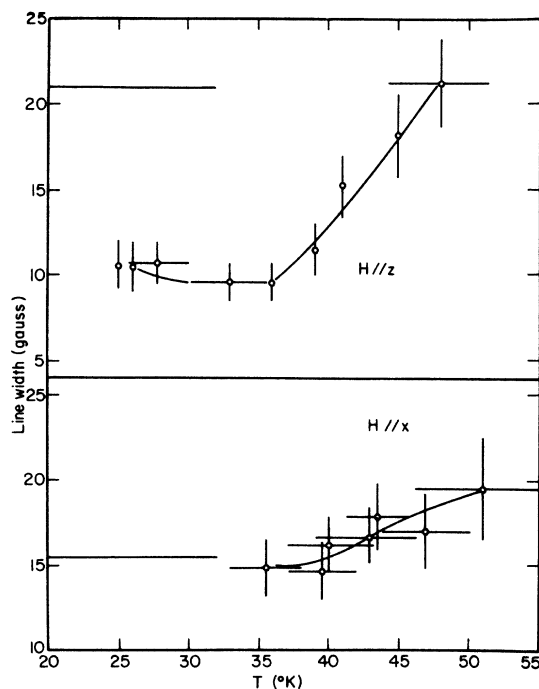


FIG. 7. Linewidth of the coalesced hyperfine spectra of Nb-doped rutile as a function of temperature. The horizontal lines are the smallest widths of the coalesced spectra expected from a simple broadening of the individual hyperfine lines.

3. Exchange Scattering with Conduction Electrons

The second process that can cause promotion of donor electrons to the conduction band is exchange scattering of the conduction electrons with the niobium donors. Such a process has been considered by Pines, Bardeen, and Slichter²⁴ as a mechanism for relaxation of paramagnetic impurities. Lepine¹¹ found exchange scattering to be the predominant hopping mechanism in P-doped Si.

The scattering process can be described by conventional collision theory in terms of

$$\Omega_{\text{ex}} = n\bar{v}\sigma_{\text{ex}}, \quad (7)$$

where the exchange scattering rate is Ω_{ex} , the concentration of conduction electrons is n , their average thermal velocity is $\bar{v} = (3kT/m^*)^{1/2}$, and the effective exchange scattering cross section is denoted by σ_{ex} . Taking the temperature dependence of n from the Hall measurements, we find that the temperature dependence of the exchange scattering rate is given by

$$\Omega_{\text{ex}} \propto T^2 e^{(-72/T)}.$$

In the temperature range of interest, this expression predicts a nearly linear relationship between $\ln\Omega$ and $1/T$, with a negative slope of 108°K .

Comparing this value with the activation energy given in Eq. (5) we find that good agreement is achieved with the exchange-scattering mechanism.

Thus, we conclude that exchange scattering is the predominant hopping mechanism responsible for the changes in the EPR spectra. We can make an order of magnitude estimate of the effective cross section. Using the experimental values at 20°K , $\Omega = 2.0 \times 10^7 \text{ sec}^{-1}$ and $n = 2.5 \times 10^{16} \text{ cm}^{-3}$; and assuming $m^* = 100m_0$,¹⁵ we obtain $\bar{v} = 3 \times 10^5 \text{ cm/sec}$. The value of the exchange scattering cross section is then found from Eq. (7); $\sigma_{\text{ex}} = 3 \times 10^{-15} \text{ cm}^2$. This value is somewhat larger than the exchange-scattering cross section estimated for Cr^{3+} in rutile¹⁵; $\sigma_{\text{ex}} = 3 \times 10^{-17} \text{ cm}^2$.

V. CONCLUSION

Our analysis of the temperature dependence of the Nb-doped rutile hyperfine spectrum has shown that the spectra cannot be explained by an increase in the spin-lattice relaxation time only. Instead, we have been able to interpret the spectra in terms of random hopping between donor sites. Only hopping via the conduction band can consistently account for all of the observed features. The dominant hopping mechanism is attributed to exchange scattering with the conduction electrons.

Although we are able to estimate an upper bound for the g factor of the conduction-electron resonance line, the exact position and width of this line still remains undetermined. We suggest it would

be useful to make a search for the conduction-electron resonance by optical pumping of the system to achieve the necessary electron populations at low temperatures. This should be done in undoped rutile, since for the Nb-doped rutile the conduction-electron resonance line is expected to be inextricably coupled to the Nb hyperfine spectra, thereby complicating any interpretation of the conduction electron spin resonance spectrum.

ACKNOWLEDGMENTS

The author is particularly indebted to Dr. Z. Sroubek for many suggestions and discussions. Special thanks are due to Dr. R. Orbach and Dr. C. A. Moore for many helpful discussions, and to J. McNeil for use of his Dial-A-Temp electronic temperature regulator.

APPENDIX

A. Absorption Spectrum for Impurity-Conduction-Band-Impurity Hopping

For the case of hopping via the conduction band, the only nonvanishing elements of matrix A are the diagonal and furthest off-diagonal elements:

$$A_{i,i} = -i(\omega - \omega_i) - \delta_i - \Omega, \quad i = 1, 2, \dots, N$$

$$A_{N+1,N+1} = -i(\omega - \omega_{\text{CE}}) - \delta_{\text{CE}} - \Omega',$$

$$A_{N+1,i} = \Omega'/N, \quad A_{i,N+1} = \Omega; \quad i = 1, 2, \dots, N.$$

Here we have identified the conduction-electron terms by the subscripts CE and $N+1$. Finding the absorption intensity we write

$$\begin{aligned} I(\omega) &= -\text{Re}(\underline{W} \cdot \underline{A}^{-1} \cdot \underline{1}) \\ &= -\text{Re} \left(\frac{1-\Delta}{N} \sum_{i=1}^N \sum_{j=1}^N (A^{-1})_{i,j} + \Delta \sum_{j=1}^{N+1} (A^{-1})_{N+1,j} \right). \end{aligned} \quad (A1)$$

We can solve for the summed terms by requiring

$$\sum_{j=1}^{N+1} \sum_{k=1}^{N+1} A_{i,j} (A^{-1})_{j,k} = 1.$$

For the case $i = N+1$,

$$\frac{\Omega'}{N} \sum_{j=1}^N \sum_{k=1}^{N+1} (A^{-1})_{j,k} + A_{N+1,N+1} \sum_{k=1}^{N+1} (A^{-1})_{N+1,k} = 1. \quad (A2)$$

For the case of $i = 1, 2, \dots, N$,

$$\sum_{j=1}^N \sum_{k=1}^{N+1} A_{i,j} (A^{-1})_{j,k} + \Omega \sum_{k=1}^{N+1} (A^{-1})_{i,k} = 1.$$

Since for $i \neq j$ the $A_{i,j}$ terms in the first summation vanish, we obtain, after rearrangement and a further summation,

$$\sum_{i=1}^N \sum_{k=1}^{N+1} (A^{-1})_{i,k} = \left(1 - \Omega \sum_{k=1}^{N+1} (A^{-1})_{N+1,k} \right) \sum_{i=1}^N (A_{i,i})^{-1}. \quad (A3)$$

Solving (A2) and (A3) for the summed terms ap-

pearing in (A1) yields

$$\sum_{k=1}^{N+1} (A^{-1})_{N+1,k} = \left(1 - \frac{\Omega'}{N} \sum_{i=1}^N (A_{i,i})^{-1}\right) \times \left(A_{N+1,N+1} - \frac{\Omega\Omega'}{N} \sum_{i=1}^N (A_{i,i})^{-1}\right)^{-1}$$

and

$$I(\omega) = -\operatorname{Re} \left\{ \frac{1-\Delta}{N} (A_{N+1,N+1} - \Omega) + \Delta \left[\left(\sum_{i=1}^N (A_{i,i})^{-1} \right)^{-1} - \frac{\Omega'}{N} \right] \left[A_{N+1,N+1} \left(\sum_{i=1}^N (A_{i,i})^{-1} \right)^{-1} - \frac{\Omega\Omega'}{N} \right]^{-1} \right\}.$$

B. Absorption Spectrum for Direct Impurity-Impurity Hopping

In the case of direct hopping from one hyperfine line to any other, the matrix elements of A for N hyperfine lines are easily seen to be

$$A_{ii} = -i(\omega - \omega_i) - \delta_i - [(N-1)/N]\Omega, \\ A_{ij} = \Omega/N, \quad i \neq j.$$

The absorption spectrum is found from

$$I(\omega) = -\operatorname{Re}(\underline{W} \cdot \underline{A}^{-1} \cdot \underline{1}) = -\frac{1}{N} \operatorname{Re} \sum_{j=1}^N \sum_{k=1}^N (A^{-1})_{jk}.$$

Since

$$\sum_{j=1}^N \sum_{k=1}^N A_{ij} (A^{-1})_{jk} = 1,$$

substitution for the off-diagonal terms in \underline{A} gives

$$\frac{\Omega}{N} \sum_{j=1}^N \sum_{k=1}^N (A^{-1})_{jk} + \left(A_{i,i} - \frac{\Omega}{N} \right) \sum_{k=1}^N (A^{-1})_{ik} = 1$$

or

$$\sum_{k=1}^N (A^{-1})_{ik} = \left(1 - \frac{\Omega}{N} \sum_{j=1}^N \sum_{k=1}^N (A^{-1})_{jk} \right) \left(A_{i,i} - \frac{\Omega}{N} \right)^{-1}.$$

$$\sum_{j=1}^N \sum_{k=1}^{N+1} (A^{-1})_{jk} = \left(A_{N+1,N+1} - \Omega \sum_{i=1}^N (A_{i,i})^{-1} \right) \times \left(A_{N+1,N+1} - \frac{\Omega\Omega'}{N} \sum_{i=1}^N (A_{i,i})^{-1} \right)^{-1}.$$

Substituting these expressions into Eq. (A1) finally gives the absorption spectrum

Summing over i and solving for

$$\sum_{j=1}^N \sum_{k=1}^N (A^{-1})_{jk},$$

we find

$$I(\omega) = -\frac{1}{N} \operatorname{Re} \left[\left(\sum_{i=1}^N [-i(\omega - \omega_i) - \delta_i - \Omega]^{-1} + \frac{\Omega}{N} \right)^{-1} \right]. \quad (\text{A4})$$

We proceed to consider the limit of $(\delta_i + \Omega) \ll |\omega_i - \omega_k|$. Restricting the values of Ω to within the neighborhood of ω_k , we find the terms in the sum appearing in Eq. (A4) not involving k to be negligible and obtain

$$I(\omega) = -\frac{1}{N} \operatorname{Re} \left(-i(\omega - \omega_k) - \delta_k - \frac{N-1}{N} \Omega \right)^{-1},$$

which is just a broadening of each hyperfine line.

If, on the contrary, $(\delta_i + \Omega) \gg |\omega_i - \omega_k|$ and $\Omega \gg \delta_i$, we find that the spectrum consists of a single narrowed line at $\bar{\omega}_i$,

$$I(\omega) = -\operatorname{Re} \left[-i(\omega - \bar{\omega}_i) - \bar{\delta}_i \right]^{-1},$$

where $\bar{\omega}_i = \sum_{i=1}^N \omega_i / N$ and $\bar{\delta}_i = \sum_{i=1}^N \delta_i / N$.

[†]Supported in part by the U. S. Office of Naval Research, Contract No. N00014-69-A-0200-4032, and the National Science Foundation.

*Present address: II. Physikalisches Institut der Technischen Hochschule Darmstadt, 61 Darmstadt, Hochschulstr. 2, Germany.

¹P. F. Chester, *J. Appl. Phys.* **32**, 866 (1961).

²G. Feher and A. F. Kip, *Phys. Rev.* **98**, 337 (1955).

³F. J. Dyson, *Phys. Rev.* **98**, 349 (1955).

⁴M. Peter, D. Shaltiel, J. H. Wernick, H. J. Williams, J. B. Mock, and R. C. Sherwood, *Phys. Rev.* **126**, 1395 (1962).

⁵T. C. Ensign, Te-Tse Chang, and A. H. Kahn, *Phys. Rev.* **188**, 703 (1969).

⁶H. P. R. Frederikse, *J. Appl. Phys. Suppl.* **32**, 2211 (1961).

⁷J. H. Becker and W. R. Hosler, *Phys. Rev.* **137**, A1872 (1965).

⁸W. R. Thurber and A. J. H. Mante, *Phys. Rev.* **139**, A1655 (1965).

⁹E. H. Putley, *The Hall Effect and Related Phenomena* (Butterworth, London, 1960), Chap. IV.

¹⁰P. W. Anderson, *J. Phys. Soc. Jap.* **9**, 316 (1954).

¹¹D. J. Lepine, *Phys. Rev. B* **2**, 2429 (1970).

¹²A. Abragam, *The Principles of Nuclear Magnetism* (Oxford,

U. P., Oxford, England, 1961), Chap. X.

¹³S. G. Barnes, J. Dupraz, and R. Orbach, *J. Appl. Phys.* **92**, 1659 (1971). The denominator of Eq. (3) is identical to the denominator of $\chi^+(\omega)$ if the molecular-field constant λ is artificially equated to zero.

¹⁴T. Goto, K. Nishimura, S. Kabashima, and T. Kawakubo, *J. Phys. Soc. Jap.* **30**, 1654 (1971).

¹⁵V. N. Bogomolov, E. K. Kudinov, S. T. Pavlov, and L. S. Sochava, *Fiz. Tverd. Tela* **10**, 2043 (1968) [*Sov. Phys.-Solid State* **19**, 1604 (1969)].

¹⁶K. A. Müller and J. Schneider, *Phys. Lett.* **4**, 288 (1963).

¹⁷The BMDX Non-Linear Least Squares Program was used to obtain the best fit. A description of this program can be found in *BMD Biomedical Computer Programs, X Series Supplement*, edited by W. J. Dixon (University of California Press, Berkeley, 1972), p. 177.

¹⁸A. Miller and E. Abrahams, *Phys. Rev.* **120**, 745 (1960).

¹⁹K. Morigaki and T. Mitsuma, *J. Phys. Soc. Jap.* **20**, 62 (1965).

²⁰K. Morigaki, S. Toyotomi, and Y. Toyotomi, *J. Phys. Soc. Jap.* **31**, 511 (1971).

²¹S. Maekawa and N. Kinoshita, *J. Phys. Soc. Jap.* **20**, 1447 (1965).

²²R. Kubo and Y. Toyozawa, *Prog. Theor. Phys.* **13**, 160 (1955).

²³H. P. R. Frederikse, *J. Appl. Phys. Suppl.* **32**, 2211 (1961).

²⁴D. Pines, J. Bardeen, and C. P. Slichter, *Phys. Rev.* **106**, 489 (1957).

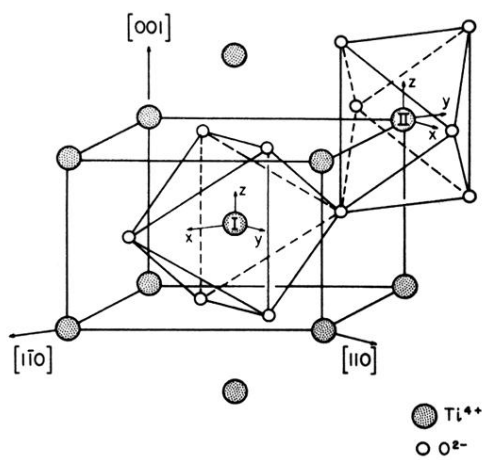


FIG. 1. Crystal structure of rutile (TiO₂). The two inequivalent sites are labeled I and II, and their magnetic axes are labeled x , y , and z .